A Neuro-automata Decision Support System for Phytosanitary Control of Late Blight

Gizelle Kupac Vianna, Gustavo Sucupira Oliveira and Gabriel Vargas Cunha

Departamento de Matematica, Universidade Federal Rural do Rio de Janeiro, BR-465, Km 7, 23897-000, Seropedica, RJ, Brazil

Keywords: Decision Support System, Cellular Automata, Pattern Recognition, Artificial Neural Networks, Digital Images Processing.

Abstract: Foliage diseases in plants can cause a reduction in both quality and quantity of agricultural production. In our work, we designed and implemented a decision support system that may small tomatoes producers in monitoring their crops by automatically detecting the symptoms of foliage diseases. We have also investigated ways to recognize the late blight disease from the analysis of tomato digital images, using a pair of multilayer perceptron neural network. One neural network is responsible for the identification of healthy regions of the tomato leaf, while the other identifies the injured regions. The networks outputs are combined to generate repainted tomato images in which the injuries on the plant are highlighted, and to calculate the damage level at each plant. That levels are then used to construct a situation map of a farm where a cellular automata simulates the outbreak evolution over the fields. The simulator can test different pesticides actions, helping in the decision on when to start the spraying and in the analysis of losses and gains of each choice of action.

1 INTRODUCTION

Over the centuries, science and technology in agronomy have been searching ways to improve productivity, in order to feed constantly growing populations, meanwhile important climatic changes affect agricultural production. An important field of research in this area is plant pathology, since many diseases affecting plants can cause economic, social and ecological losses. In this context, it is very important to have a quick and accurate diagnosis of diseases to which a plant is susceptible.

In Brazil, where an important part of the economy depends on agriculture, it is essential that farmers maintain a strict control over the quality of their crops. In 2015, the agribusiness corresponded to 21.46% of the Brazilian GDP, or more than US$400.00 million (IBGE, 2016; MAPA, 2016). Particularly, the tomato (Solanum lycopersicon) crop occupies the seventh position in the rank of food plant tons produced per year, with more than 1.9 tons produced in 2014 (IBGE, 2016). However, that plant is vulnerable to many diseases and requires extreme care in terms of fertilization and phytosanitary treatment, ranking the second position in pesticide consumption per planted area in Brazil

(Neves et al., 2003), where tomatoes are typically produced in small farms and require continuous monitoring from experts, which might be prohibitively expensive and time-consuming. Thus, the search for fast, less expensive and accurate methods to detect the foliage diseases is of great significance.

Many studies show the impact of plant diseases over the quality of agricultural products (Zamberlan et al., 2014; Tilman et al., 2002; Rembialkowska, 2007). The most common disease that affects tomato crops worldwide is the late blight, a very damaging disease also widespread in Brazil. The tomato late blight is caused by *Phytophthora infestans*, a fungus that inhabits the soil and disseminates through spores. The disease occurs especially in cold and humid months when the dispersion of spores is facilitated by wind and high humidity, and they reach the leaves, fruits, and branches, where they germinate, producing a new infection focus. The disease can spread quickly, specially under favorable climatic conditions consisting of a combination of relative humidity under 90% and temperature around 20°C (68°F). As a result, we have an epidemic that can lead to considerable losses in production (Mizubuti et al., 2002; USDA, 2016).

481

On the other hand, the indiscriminate use of pesticides in tomato fields brings serious problems not only to human health but also to the environment. Moreover, pathogens have started developing resistance to the conventionally used fungicides and a second generation of more expensive fungicides began to be used. Therefore, it is critical to use fungicides in proper doses and intervals (Saxena et al., 2014; Goufo et al., 2008; Zhang et al., 2013; Park et al., 2014).

The goal of this paper is to present a novel computer-based solution that may help farmers to make better decisions to combat late blight on tomato crops, expanding previous works (Vianna and Cruz, 2013a; Vianna and Cruz, 2013b). This research aims at helping the detection of late blight in tomato crops, and the measuring of the damage level at each plant, by using a pattern recognition system based on multilayer perceptron neural networks (MLP). We also developed a decision support system that generates simulations of spreading scenarios of contamination and tests alternatives for combating the disease, supported by meteorological data and prediction models of the late blight.

2 INFORMATION TECHNOLOGY IN AGRICULTURE

Agriculture production systems have frequently benefited from the incorporation of technological advances and with the aid of information technology for early detection of crop diseases, it was possible to delay the beginning of pesticides spraying in comparison with the fixed schedule spraying method (Zhanga et al., 2002; Sankaran et al., 2010; Mahlein et al., 2012). We can find examples in the literature where results obtained by monitoring the spores of tomato late blight in the air allowed producers to obtain an average reduction of 50% in total sprays, reaching rates of 80% reduction in some cases (Bugiani et al., 1995).

2.1 Pattern Recognition in Diagnosis of Tomato Diseases

Farmers and workers visually recognize the disease by the appearance of dark brown lesions on tomato leaves that vary from brown or grey to pale green, often situated at the edges of the leaves (Correa et al., 2009).

In Brazil, the most common approach used in the fight of the disease involves naked eye observations and manual classification of the degree of infestation at each plant. This classification is based on a visual comparison between the infested leaf and some schematic images of tomato leaves that quantify the degree of infestation in a logarithmic scale (Correa et al., 2009). After analyzing some samples of plants from the farm, the mean of infestation degree at each sample is used to define a schedule of pesticide spraying.

2.2 Digital Approaches for Analysis of Plant Leaves

Image processing is a useful tool for analysis in various agricultural applications and several studies have also investigated the use of broadband color, or chromaticity values, for plant species recognition (Sankaran et al., 2010; Barbedo, 2013; Vibhute and Bodhe, 2012; Bock et al, 2010). One of the key advantages of these techniques is that pixel-based color classifiers tend to be less computationally intensive than shape-based methods (Nixon and Aguado, 2008). In this paper, we used the color tones from individual pixels of the leaves to classify them in one of the seven possible degrees of the scale from (Correa et al., 2009). The images were captured directly from the field, and so it is expected that they contain a significant amount of noise from the background and shadows. We used a mean filter to reduce the details of abrupt color changes, which improved the performance of our pattern classifier.

3 MATERIAL AND METHODS

3.1 Processing of Digital Images of Leaves

At the beginning of this research, we decided to provide our target users with the free use of our classification system. In addition, as they are small farmers, they may not afford expensive equipment or might be unable to operate it properly. Thus, we have not used any sophisticated machinery or proprietary software packages to lower the cost of the final system. Based on that premise, we worked upon digital images obtained by low-resolution built-in cell phone cameras. The pictures were taken in an open environment under natural sunlight conditions in the experimental fields of the Horticulture Department of our institution in a

cropping area historically linked with the natural occurrence of late blight.

We used a combination of two ANN's to perform, for each pixel, its classification into one of three possible categories: healthy, injured or background. After classifying all the pixels of one single image, we used the class information of all these pixels to compute the final classification of the whole leaf, assigning it a degree of contamination, as defined in (Correa et al., 2009).

In the sequence of processes performed over the digital images, the first step was to reduce the definition, achieving 70% of the original size, to speed up the performance of further procedures. After that, for each image, we generated a text file that contained, for each pixel, the X-Y coordinates of the pixel and its RGB and HSL values. Next, all variables were linearly normalized, generating a new data table containing RGB and HSL values, varying from 0 to 1, which suits better to the training process of an ANN. We chose that normalization technique because the variable scales are similar (R,G, and B varies from 0 to 255; H vary from 0 to 359; S and L varies from 0 to 100) and because, as the domain is limited, there is no possibility of occurring outliers.

3.2 Pattern Recognition System

We conducted an experiment using two different ANNs. The first ANN was trained to recognize green tones of the leaf or, in other words, healthy pixels. If a pixel was recognized as healthy, the ANN answer would be 1 (class 1), but if it was considered as belonging to the non-healthy class, the ANN answer should be 0 (class 0). The training of the latter ANN was similar, but it was conducted to recognize brown tones of the leaf, or injured pixels. For the ANN's training, we fist chose some pixels from specific areas of our available pre-processed images. Each image can give us around 1,500 pixels, and we have used no more than four images to construct the training subset for the ANN's, where each record contained the color information plus the class label. The classification of each pixel considers the values of their R, G and B components from the RGB color system plus H, S, and L components from the HSL color system. We selected over 6,000 different labelled pixels, where around 2,000 came from each class. The classes could be green (corresponding to the different green tones a healthy leaf could have), red (the different brown tones a leaf affected by late blight could have), or background (which includes earth, sky, sticks and other noise colors). Examples of healthy, injured and

backgrounds pixels are shown in Figure 1.

After labelling each pixel according to their classes, the three datasets were joined, shuffled, and linearly normalized, as explained above. We divided the resulting dataset in a 5:2 proportion, and then circa 5,000 records were used for the pair of ANN's training and around 2,000 for testing them.

We have evaluated many ANN configurations, varying the learning rate from 0.4 up to 0.8 (with steps of 0.2), the momentum from 0.5 up to 0.9 (with steps of 0.2), and the number of hidden neurons from 4 up to 20, for one or two hidden layers of neurons. We have also tested different activation functions (such as hyperbolic tangent, sigmoid and purelin) in different combinations through the neuron layers.
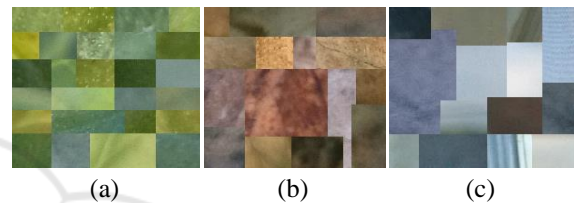

(a)   (b)   (c)

Figure 1: Each image shows one subset of pixels used to train the pair of ANN´s. Each subset corresponds to one different class and was built by pixels extracted from digital images of tomato leaves (a) Green: pixels from healthy areas of the leaves, (b) Red: pixels from injured areas and (c) background pixels.

Each different configuration was trained and tested 20 times to find the best one in average, in a total of 1,728 different ANN models. For each training, we randomly choose 1,200 records from our labelled training dataset. Similarly, for each test, we randomly selected 500 labelled records from the testing dataset.

Finally, we chose the configuration with the best performance for each ANN. For the *green*-ANN, the best configuration was the 16-8-1 network, with training rate equal to 0.8, *momentum* equal to 0.9, and sigmoid activation function at all levels and a value of 0.5 for the threshold between the outputs. After analysing each network from the total amount of 20 networks trained and tested with this configuration, we chose to use the one that achieved the best accuracy rate, which was a rate of about 97.99% in correct pixel classification. For the *red*-ANN, the best configuration was the 16-16-1 network, with training rate equal to 0.6, *momentum* equal to 0.7, and sigmoid activation function at all levels and the same value of 0.5 for the threshold. For that configuration, we chose the one with a rate of about 97.92% in correct pixel classification.

The proposed approach used an Intel(R) Core(TM) i7-3517U CPU, 1.90GHz, and 6GB RAM, with an Intel(R) HD Graphics Family card for developing and running the system, and only free license softwares: Eclipse IDE for Java and free packages such as Neuroph (Sevarac, 2012), AWT Image, Java Advanced Imaging (JAI), plus the MySQL as the relational database system. The images were taken in an experimental field using a built-in cell phone camera; the resolution of the images was reduced to only 0.3 megapixels, and each image file was less than 100 KBytes.

4 THE NEURAL NETWORK CLASSIFIER

After the training phase, we tested the ANN system with 60 new different leaf images. First, each image was pre-processed, having its definition reduced and being mean-filtered, as explained above. Second, for each image, we extracted the x and y coordinates and the RGB and HSL values of each pixel, and those data were stored in a different file for each image. Last, each record of a file was presented to the pair of ANN's and classified by it. This final step generates a new file, containing, for each pixel of the original image, its x and y coordinates plus its final classification.

The final classification of each pixel from one single image was used to reconstruct the leaf image, and converted into a three-colored codification, where the new image contains only green, red or black pixels. During the conversion processes, we also calculated the ratio of red pixels over green pixels for each image. That ratio was then used to define the degree of late blight infestation of each leaf, as shown in (1):

$$injured\ level = \frac{number\ of\ injured\ pixels}{total\ number\ of\ leaf\ pixels} \times 100 \quad (1)$$

In (1), the *total number of leaf pixels* accounts only for pixels belonging to the leaf itself (healthy plus injured), despising all background pixels, whereas the *injured level* indicates the percentage of injured areas over one leaf. We did not count black pixels, as they were not relevant to the final goal, which is to discover the damage extension of the leaf. The injured level was then used to assign, for each image, a status number, as shown in Table 1. That status represents the health condition of the corresponding tomato plant and Figure 2 shows some examples of original images and their respective codified images.
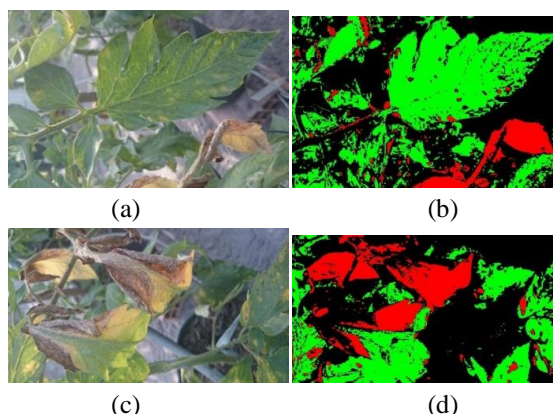

(a)   (b)

(c)   (d)

Figure 2: Examples of injured leaves from tomatoes, taken in our experimental field, infected by P. infestans. The images illustrate the images before and after the classification process. Figure (2a) was accounted as having a 15% of damage, or status 2, whereas Figure (2d) was accounted for 32%, or status 4. It is important to notice that the account was made considering the whole group of leave captured by the camera, which was considered to belong to the same plant.

Most of the pictures processed by the system have a considerable number of background elements that cause interference on the classification process. Even after we reduced the noise by the mean-filtering process, these background elements remained, sometimes with the same color tonalities of the healthy areas, and sometimes with the same color tonalities of the sick areas of the plants. As our goal is to use a drone to take the photos in the future so we will try to deal automatically with those problems in our next studies.

Table 1: Status for each range of damage percentage (Correa et al., 2009).

Status	0	1	2	3	4	5	6
% of damage	= 0	0-3	3-12	12-22	22-40	40-76	>=77

5 THE DECISION SUPPORT SYSTEM

According to the Integrated Pest Management Program of California University (UCIPM, 2016), there are several reputable prediction models of late blight propagation in tomato and potato crops. Among those, we have chosen the Hyre prediction model (Hyre, 1954) that indicates that an initial outbreak of late blight will occur between 7 to 14 days after 10 consecutive favorable days. A

favorable day, in turn, occurs after five consecutive days where the mean temperature stays between 7.0°C and 25.5°C (48°F and 78°F) and, at the same time, after 10 days with a total precipitation equal to, or higher than, 30 millimetres (1.2 inches).

5.1 The Forecasting Model

A forecasting model should perform multi-day simulations and, for that reason, we needed to use up to 40 days of meteorological prediction. To solve that requirement, we have used historical data obtained through the National Institute of Meteorology (INMET, 2016). We have used that data to calculate the mean of some meteorological variables in specific periods of the year, chosen by the system user during the simulation. We tested the system with data from the city of Paty do Alferes, because this is the main tomato producer region in the State of Rio de Janeiro. Thus, we collected some meteorological data from that region from 01/01/1999 until 01/01/2015, which includes temperature, relative humidity, minimum temperature, maximum temperature and precipitation.

The system user can choose the size of the data window that will be used in the historical average calculation, and it can be 5, 10 or 15 years, for all available variables. Finally, those historical averages are used to estimate the meteorological variables, required for Hyre's model, for each day of the period of simulation, as exemplified in Table 2.

5.2 The Cellular Automata Model

We have used a cellular automata (CA) to model the dynamics of late blight, defined in the two-dimensional domain, with Moore's neighbourhood and a probabilistic transition function based on Hyre's prediction model.

Table 2: Example of calculation of the expected temperature for June 6th, 2016, using the historical average temperatures and a 5-years window.

Simulation Iteration	2010	2011	2012	2013	2014	Average Result
06/06/16	17.42	11.24	21.64	18.48	16,88	17,13

The CA works over a matrix that represents a cultivated area of tomatoes where the columns correspond to lines of the cultivated area. Within each column of the matrix the tomato plants are arranged through the rows. Coherently, each cell in the matrix represented a tomato plant that has a health condition value, or status, associated with it.

The user defines the variable CA parameters, as the *size* of the historical data window and the *wind direction*. The parameter *wind direction* controls the direction of the status changes. The status of any cell would only change if it can be reached by an infected cell in its neighbourhood and if the wind direction allows this contact.

For each cell of the matrix, we calculated its status in the next iteration by analysing the current status of all its neighbors. The next status of a cell $c(i,j)$, where i is the line and j is the column, depends on its current status, $E(c(i,j))$, and on the current status of all its neighbors, in a neighborhood of size 8. An infected cell could have its status worsened when there are infected cells in its neighbor, or improved, when a technique C for combating the disease is being used. Each neighbor can affect a cell $c(i,j)$ in a weighted way, according to the factors indicated by Hyre's model. The weighted influence of each neighbor is calculated following the rules shown in Table 3, which considered the number of outbreaks Qo, the number of favorable days Qf, and the current status E of cell $c(I, j)$. Each cell in a neighborhood would also change its value in the next step, and the combination of all changes would build the new status matrix.

We have tested two forms of combat and, according to the literature (Rebouças et al., 2014), the combat type 1, which uses Dimethimorph, could decrease the status of a cell by 30% of the current status. On the other hand, combat type 2, which uses Metalaxyl-M+Mancozeb, could decrease the status by 20%. Thus, when using a combat method, the CA dynamics can be summarized by (2) and Table 3.

$$E'\big(c(i,j)\big) = E(c(i,j)) + \sum_{n=1}^{8} P\big(v_n(c(i,j))\big) - C * E(c(i,j)) \quad (2)$$

Table 3: Rules for calculation of weight P.

		1	2	3	4	5	6
Qs> 1	Qd> = 10	0.1	0.8	1.4	1.6	1.8	2
	10> Qd> = 7	0.1	0.5	1	1.1	1.2	1.4
Qs> 3	7> Qd> = 5	0.2	0.4	0.6	0.7	0.8	0.9

6 RESULTS AND DISCUSSION

The rules that control the simulation dynamics, altering the cells status in order to represent the spreading of late blight in the field are defined by a set of parameters adjusted according to the Hyre's model.

The simulation system is capable of mapping the streets and lines of a farm, registering images and georeferences of infected tomatoes. It can simulate scenarios of contagion spreading in a determined period from 10 up to 200 days. It is also possible to stop the simulation at any time to choose a combat method for the disease and then resume the simulation. The system main functions are the module for processing and classification of digital tomato images described in previous sections, and the simulator that generates scenarios of spreading of contamination and alternatives to combat the disease.

In the module for processing and classification, the images are classified within the status scale. Thus, they are placed in a matrix based on their real georeference information and the cell is painted with a different color for each different status (Table 4).

The resulting matrix thus conceptually represents a map of the cultivated area being monitored by the system (Figure 3a). In the map, it is possible to select any cell and retrieve the corresponding sample information, including the original leaf image, the current health condition of the plant and the location of the plant in the field (Figure 3b).

In the simulation module, it is possible to run simulations of late blight spreading and visualize it in the conceptual map of the cultivated area. It is also possible to analyse strategies to combat the disease. The simulation is interactive and simple, and the user can pause, resume or restart the simulation at any stage (Figure 4).

If a combat is tested during the simulation, a new dynamic could occur, reducing the status of tomatoes, depending on the contamination level of the field as a whole, the climatic factors, and the type of combat chosen. Figure 5 shows what happens when combat type 2 is used on the 12th day of simulation.

Table 4: correspondence of map cells for each possible status.

Status	0	1	2	3	4	5	6
Cell color	Dark green	Green	Light green	Yellow	Orange	Dark Orange	Reddish orange

Starting from the same situation of Figure 4a, it is possible to see that the losses could be minimized in the end of the 30th day of simulation.
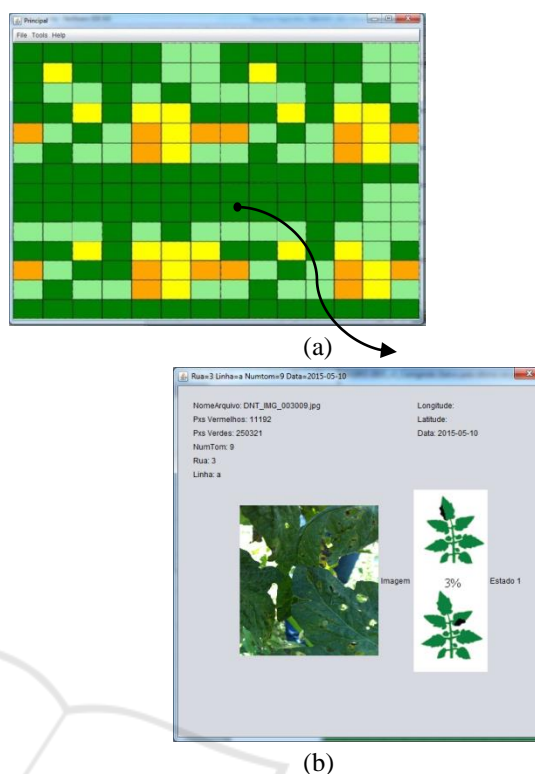

(a)

(b)

Figure 3: (a) Conceptual map of a cultivated area of tomatoes from a monitored farm. (b) Details from a selected tomato on the map.

Our approach was to convert the original JPEG images into codified red/green images, what proved to be effective in highlighting the injuries of the leaves (Bock et al., 2010). On the other hand, the codification process was able to overcome problems such as low resolution, focus, and image blur of the digital images, with no need to use more sophisticated digital image algorithms (e.g. contour detection).
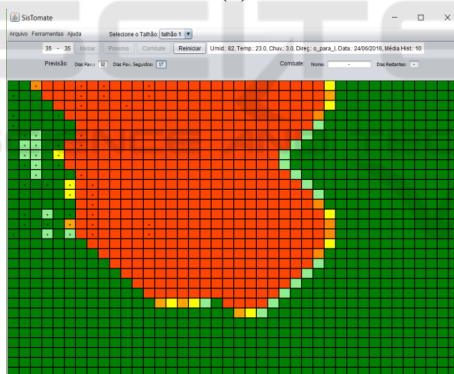
Since we have worked with images captured in the field, in natural sunlight and taken by cell phones cameras, it was expected that they would contain a large amount of noise. As future work, we will include more image filtering processes, aiming at noise removal or attenuation.
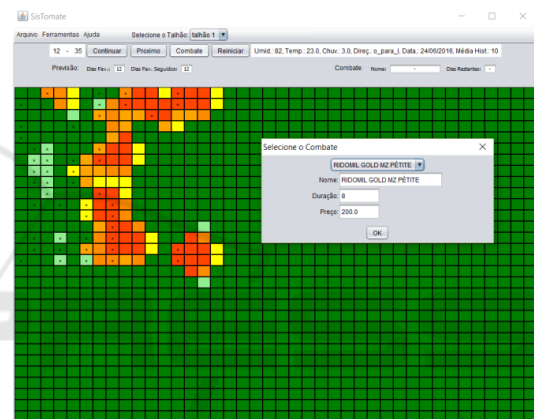
(a)
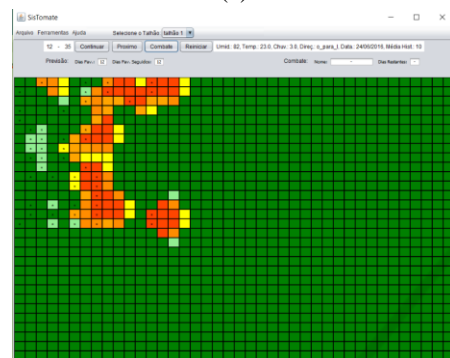
(b)

(c)

Figure 4: A non-combat simulation starting at 06/24/2016, having wind direction from west to east and conducted during 35 iterations on a matrix with 1200 elements, where each cell represents one tomato plant. (a) At the beginning, before the simulation starts, with cells containing the original status of each plant, collected *in loco* (cells marked with an '*' represents one photographed plant, while the others have their status all settled to 0-healhy); (b) The map situation at iteration number 12, which means that the map represents the farm situation after 12 days from the initial day (c) The map situation at the 35th day, when the simulation ends.

We are already working on a panel of statistics that will show the performance of the simulation,

displaying the financial results obtained by chosen a specific combat strategy, and comparing the costs of using the pesticides against not using at all.

The alternative we presented can accelerate the identification of the disease and help measuring the extension of the infestation. Plus, it can help small farmers to plan better the best time for spraying fungicides, protecting the environment while reducing the plantation costs.

We have modelled the dynamics of two chemical fungicides to be available in this first version of our simulator because they are the most common in Brazil for tomato blight control. However, it is relatively simple to model new chemical control methods, and we are working on a tool that enables the user to do so.

(a)
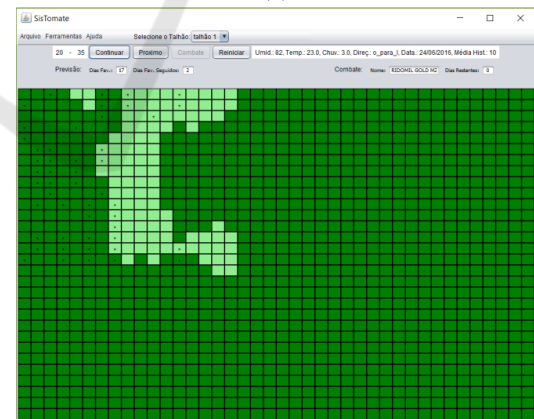
(b)

Figure 5; A combat type 2 simulation starting at 06/24/2016, having wind direction from west to east and conducted during 35 iterations on a matrix with 1200 elements, where each cell represents one tomato plant. (a) On the 12th day of simulation, the combat type 2 was selected and the simulation was resumed; (b) The map situation at iteration number 35, when the simulation ends.

REFERENCES

Barbedo, J., 2013. Digital image processing techniques for detecting, quantifying and classifying plant diseases. In *SpringerPlus*, 2:660.

Bock, C., Poole, G., Parker, P., Gottwald, T., 2010. Plant disease severity estimated visually, by digital photography and image analysis, and by hyperspectral imaging. In *Critical Reviews in Plant Sciences*, vol. 29, n. 1-3, pp.:59–107.

Bugiani, R. et al., 1995. Monitoring airborne concentrations of sporangia of Phytophthora infestans in relation to tomato late blight in Emilia Romagna, Italy. In *International Journal of Aerobiology*, vol. 11, , pp.:41-46, Elsevier Science.

Correa, F., Bueno, J., Carmo, M., 2009. Comparison of three diagrammatic keys for the quantification of late blight in tomato leaves. In *Plant Pathology*, vol. 58, pp.:1128-1133.

Goufo, O., Mofor, T., Ngnokam, D., 2008. High Efficacy of Extracts of Cameroon Plants Against Tomato Late Blight Disease. In *Agronomy for Sustainable Development*, vol. 8, INRA, EDP Sciences, pp.567-573.

Hyre, R., 1954. Progress in forecasting late blight of potato and tomato. In *Plant Disease Reporter*, Illinois, vol. 38, n.4, pp.: 245-253.

IBGE, 2016. *Sistema IBGE de Recuperação Automática – SIDRA*. [online] Available at: http://www.sidra.ibge.gov.br/bda/agric/default.asp?z=t&o=11&i=P [Accessed 18 Oct. 2016].

INMET, 2016. [online] Available at: http://www.inmet.gov.br/portal/ [Accessed 5 Jun. 2016].

Mahlein, A., Oerke, E., Steiner, U., Dehne, H., 2012. Recent advances in sensing plant diseases for precision crop protection. In *European Journal of Plant Pathology*, vol. 133, n.1, pp.:197-209.

MAPA, 2016. *Estatísticas e Dados Básicos de Economia Agrícola*. [online] Available at: http://www.agricultura.gov.br/arq_editor/Pasta%20de%20Setembro%20-%202016.pdf, [Accessed 10 Oct. 2016].

Mizubuti, E., Maziero, J., Maffia, L, Haddad, F., Lima, M., 2002. CGTE Program: Simulation, Epidemiology and Management of Late Blight. In *Global Initiative on Late Blight Conference*, Hamburg, Germany.

Neves, E., Rodrigues, L., Dayoub, M., Dragone, D., 2003. Bataticultura: dispêndios com defensivos agrícolas no quinquênio 1997-2001. In *Batata Show*, vol. 6, pp. 22-23.

Nixon, M., Aguado, A., 2008. *Feature Extraction and Image Processing*, 2nd Ed, Elsevier Ltd.

Park, D., Zhang, Y., Kim, B., 2014. Improvement of resistance to late blight in hybrid tomato. In *Hort. Environm. Biotechnol*, vol. 55(2), Springer, pp.:120-124.

Rebouças, T. et al., 2014. Potencialidade de Fungicida e Agente Biológico no Controle da Requeima do Tomateiro. In *Horticultura Brasileira*, vol.32(01).

Rembialkowska, E., 2007. Quality of plant products from organic agriculture. In *J. Sci. Food Agric.*, vol. 87, pp.:2757–2762.

Sankaran, S., Mishraa, A., Ehsani, R., Davis, C., 2010. A review of advanced techniques for detecting plant diseases. In *Computers and Electronics in Agriculture*, vol. 72, n.1, pp.:1-13.

Saxena, A., Sarma, B., Singh, H., 2014. Effect of Azoxystrobin Based Fungicides in Management of Chilli and Tomato Diseases. In *Proced. National Academy of Sciences*, India:Springer.

Sevarac, Z., 2012. *Neuroph - Java neural network framework*. [online] Available at: http://neuroph.sourceforge.net/ [Accessed 10 Jan. 2012].

Tilman, D. et al., Agricultural sustainability and intensive production practices, 2002. In *Nature*, Aug 8, 418(6898), pp.: 671-677.

UCIPM, 2016. [online] Available at: http://www.ipm.ucdavis.edu/DISEASE/DATABASE/potatolateblight.html [Accessed 9 Jun. 2016].

USDA, 2016. *USABlight Project*, [online] Available at: https://usablight.org/node/29 [Accessed 4 Oct. 2016].

Vianna, G., Cruz, S., 2013a. Análise inteligente de imagens digitais no monitoramento da requeima em tomateiros. In *Anais do IX Congresso Brasileiro de Agroinformática*. Cuiabá, Brazil.

Vianna, G.K., Cruz, S., 2013b. Redes neurais artificiais aplicadas ao monitoramento da requeima em tomateiros. In *Anais do X Encontro Nacional de Inteligência Artificial e Computacional (ENIAC)*, Fortaleza, Brazil.

Vibhute, A., Bodhe, S.K., 2012. Applications of image processing in agriculture: a survey. In *International Journal of Computer Applications*, vol. 52, n.2, pp.:34-40.

Zamberlan, F. et al., 2014. Produção e manejo agrícola: impactos e desafios para sustentabilidade ambiental. In *Engenharia Sanitária Ambiental*, Edição Especial, pp. 95-100.

Zhang, C. et al., 2013. Fine mapping of the Ph-3 gene conferring resistance to late blight (Phytophthora infestans) in tomato. In *Theor. Appl. Genet.*, vol. 126, Springer-Verlag, pp.:2643-2653.

Zhanga, N., Wangb, M., Wanga, N., 2002. Precision agriculture-a worldwide overview. In *Computers and Electronics in Agriculture*. vol. 36, issues 2-3, pp.:113-132.